

## BUBBLING FLUIDIZED BED COMBUSTOR

ALY KAMEL ABD EL-SAMED

*Mechanical Power Engineering Department, Faculty of Engineering, Suez Canal University, Port-Said, Egypt.*

### دراسة احتراق حبيبات الفحم والخشب في فرن ذو وسادة هوائية مميعة

تم تصميم وتصنيع فرن ذو وسادة هوائية مميعة لبحث مدى إمكانية استخدام حوائط الفرن كمصدر أساسي للتسخين وإمكانية الاستغناء عن الإنابيب المغموسة في حبيبات الفحم والتي كثيراً ما تتعرض لمشكلات التآكل . كذلك مدى إمكانية استبدال الحبيبات الخاملة والتي تستخدم كمصدر لتخزين الحرارة ولتسخين حبيبات الوقود بقوالب من الطوب الحراري مبطن للفرن من الداخل.

تم إجراء تجارب عملية لاحتراق حبيبات الفحم بمقاسات مختلفة تتراوح من 1.7 ، 3.7 ، 5.5 ، 9 ، 17 مم عند سرعة هواء 1 متر/ثانية. تم تسجيل نتائج قياسات كلا من : درجات حرارة الغازات على طول محور الفرن وكذلك عند الجدران، معدل تدفق الحرارة، معامل انتقال الحرارة إلى جدران الفرن وكذلك مستوى احتراق الفحم . ولقد وجد أن أكبر قيمة لمستوى احتراق حبيبات الفحم تم التوصل إليها عندما كان متوسط قطر حبيبات الفحم 17 مم. وأن متوسط معدل انتقال الحرارة إلى الجدران 142 كيلوات/متر<sup>2</sup> .

وبعمل مقارنة بين حبيبات فحم المنارة المصري ونشارة الخشب وجد أن مقدار متوسط معامل انتقال الحرارة في حالة احتراق الفحم (1050 وات/متر<sup>2</sup> درجة) خمسة مرات نظيرة في حالة احتراق نشارة الخشب. يمكن استخدام هذا النظام في توليد الطاقة بحرق العديد من أنواع الوقود الرديء والمخلفات وكذلك التخلص من البقايا العضوية المضرّة بالبيئة وذلك بتفعيل الحرق المشترك "وقود وبقايا عضوية و مخلفات صلبة".

#### ABSTRACT

A Bubbling Fluidized Bed Combustor (BFBC) is designed and set-up to investigate the combustion processes of sub-bituminous Egyptian coal particles and wood. The effect of changing the coal particles size, with keeping the fluidized air velocity constant, on: gas temperatures, heat flux to the combustor wall, radiant-convective overall heat transfer coefficient and combustion level of coal particles is investigated.

The highest combustion level is found at coal particles size of 17 mm. The heat transfer coefficient in the case of coal combustion is extremely greater by 500% than that of wood combustion.

**KEYWORDS:** Combustion, Fluidized bed, Egyptian Coal, wood.

#### 1. INTRODUCTION

Fluidized Bed Combustion (FBC) is a leading technology for the combustion of a range of fuels [1&2], fossil and others, because of several inherent advantages it has over conventional combustion systems including fuel flexibility, low NO<sub>x</sub> emissions, in situ control of SO<sub>2</sub> emissions [3], excellent heat transfer, high combustion efficiency, and good system availability. The

development of the fluidized bed concept started in 1922 for gasification of lignite [4]. In the 1950s, the pioneering work on coal-fired fluidized bed combustion started in Great Britain [5]. Application of fluidized bed for the incineration and co-firing began in 1960 [6].

The fluidized bed boiler represented a potential lower cost, more effective, and cleaner method to burn coal. In a typical FBC system, coal, an inert

material such as sand or ash, and limestone are kept suspended through the action of combustion air distributed below the combustor floor. Fluidization depends largely on the particles size and air velocity [7-9]. Combustion experiments were carried out to evaluate a suitable combustion coal-chars reaction rate model [10]. Ignition tests were conducted with a high volatiles bituminous coal [11] and their blends in bench scale fluidized bed combustor [12].

Although FBC offers a number of significant advantages, there are also some disadvantages with the technology. In most bubbling fluidized bed combustor (BFBC), heat transfer surfaces include immersed tube banks in the dense bed [13-15], water walls in the dense bed, and tubes in the convective pass. Corrosion of metal components immersed in the bed at metal surface temperatures of 500°C and above was recorded [15]. At metal temperatures in excess of 650°C, the corrosion can be severe, especially in the presence of limestone [16]. The disadvantages also, include the necessity for handling large amounts of solids: fuel, limestone, and inert bed material.

To eliminate the effect of these disadvantages, the present work is carried out to investigate the validation of: (1) the usage of the combustor wall as a heat transfer receiver in the free board section rather than the immersed tubes in the dense bed which exposed to corrosion, (2) The usage of refractory bricks which lined the bed and act as a thermal flywheel, rather than the large amount of the inert bed material. The effect of changing the coal particles size (0.7, 1.7, 3.7, 5.5, 9, and 17 mm) with keeping the fluidized air velocity constant (1 m/s) on: gas temperatures, heat flux to the combustor wall, radiant-convective overall heat transfer coefficient ( $h_{R.C}$ ) and combustion level of coal particles is investigated.

## 2. THE EXPERIMENTAL SET UP

The bubbling fluidized bed combustor (BFBC) is a vertical steel vessel with the following major components as shown in Fig.1-A: (1)- a fluidized bed of the coal particles, which is lining with refractory bricks (7) such that the net inner square section is 17cmx17cm, (2)- a free board section, in which most volatile matters burns, (3)- A plenum or windbox, into which fluidizing combustion air is received, (4)- an air distribution plate, which transmits the combustion air from the windbox to the fluidized bed uniformly, (5)- a cyclone vessel, (6)- a screw feeder of the coal particles, which is provided with a vibrator to provide overfeed steady flow. The combustor is surmounted by a conical hood 15cm height. The flue gases are led up through the conical hood to the cyclone unit where fly-ash trapped in the ash collector (8), while the flue gases exhausted from the exhaust stack (11). The free board section is pierced with a glass window (10) and seven ports for insertion of water cooled measurements probes to measure gas temperatures and heat flux to the combustor wall. The ports are drilled along the free board in the vertical direction.

The combustion air is supplied (12) from an air blower to the windbox (3) through two opposite tubes of 7.5 cm diameter baffled apertures located at different levels to ensure swirling and uniform upward air-flow into the combustor bed. As the air velocity is increased through the bed, there is a point at which the gas-air drag force overcomes the force of gravity on the coal particles. At this point, the inter-particles distance increases, the bed expands, and the particles appear to be suspended in the gas/air stream. This is the onset of fluidization, and the air velocity at this point is referred to as the minimum fluidizing velocity. Bubbles passing through the bed occupy 20-50% of the bed volume and give intensive agitation and mixing of the bed particles [17]. Many preliminary trials are done to determine the suitable operating conditions. The suitable static head of the coal particles bed is found to be

3 cm and the fluidized air velocity is found to be 1 m/s enough to achieve the fluidization to the coal particles.

Four gas burners, at the top of the bed, are used in order to heat up the refractory bricks uniformly. When the air temperature is reached 500°C at the fluidized-bed, the four burners are shut down and the calibrated coal particles are fed uniformly onto the distributor plate meanwhile, the combustion air is flowed and distributed underneath the particles. After completion of coal feeding, one of the burners is re-lighted to ignite the coal particles. Once the coal particles are ignited, the burner is shut down and combustion of coal particles continue with the help of the thermal flywheel effect of the refractory bricks. Combustible gases leave the bed (1) and pass through the freeboard (2) to complete their combustion there, where char-coal particles entrained in the gases fall back by gravity to be fluidized in the bed.

A vertical thermocouple probe (13) is let down from the top of the combustor to measure the centerline gas temperatures along the free board at different incremental levels. Gas temperatures are not measured at the bed section (1) because of the continuous breakage of the thermocouple junction due to particles impingement and also, the high fluctuation of the gas temperature values due to the effect of bubbling burst.

The combustor free board section (2) acts as integral afterburner, where released volatile matters are burnt followed by the combustion of lighter char-coal particles which significantly are burnt for longer residence time.

The combustor is logged with thermal insulation to minimize the heat loss to surrounding.

Measurements of gas temperatures along the combustor centerline and near the wall are measured using fine thermocouples wires (Platinum and 13% Platinum-Rhodium) of 100  $\mu\text{m}$  diameters. The fluidized air velocity is measured using

thermal anemometer which is used to calibrate U-manometer.

A heat flux meter, as shown in Fig.1-B, is designed and manufactured from steel such that its circular cross section area equal 1  $\text{cm}^2$  and the distance between the two junctions of the thermocouples is 5 cm. The top of the meter must be surfacing to the inner wall of the combustor when measuring the heat flux. Conducted heat transfer through the combustor wall could be determined from the following equation by substitute the measured temperature difference along the heat flux meter;

$$\text{heat flux} = \frac{k \cdot \Delta T_x}{x} \quad \text{W/m}^2$$

$k$  = thermal conductivity of the metal of the heat flux meter,  $\text{W/m} \cdot ^\circ\text{C}$

$\Delta T_x$  = differential temperature along the heat flux meter,  $^\circ\text{C}$

$x$  = longitudinal distance,  $\text{m}$

### 3. CALCULATIONS

#### 3.1. Radiant-Convective Overall Heat Transfer Coefficient ( $h_{R-C}$ )

The obtained flames are high luminous because of the incandescent solid, char-coal, particles. The heat transfer to the combustor wall is occurred as a result of; radiant heat transfer from the char-coal particles, radiant from combustion gases products and convection heat from gases. The following equations are re-arranged:

- Radiant heat transfer from particles-flame,  $q_{R-flame}$

$$q_{R-flame} = \sigma \epsilon_f \epsilon_w (T_p^4 - T_w^4) \quad \text{W/m}^2$$

where:

$\sigma$  = Stefan-Boltzmann constant ( $5.669 \times 10^{-8} \text{ W/m}^2 \cdot \text{K}^4$ )

$T_p$  = absolute temperature of the char-coal particles or flame,  $\text{K}$ ,

$T_w$  = absolute temperature at the wall,  $\text{K}$ ,

$\epsilon_f$  = emissivity of the flame,

$\epsilon_w$  = emissivity of the wall,

- Radiant heat transfer from gases,  $q_{R-gas}$  for grey enclosure,

$$q_{R-gas} = \sigma \left( \frac{\epsilon_w + 1}{2} \right) (\epsilon_g T_g^4 - \alpha_g T_w^4) \quad W/m^2$$

where:

$\epsilon_g$  = emissivity of the gases at  $T_g$ ,

$\alpha_g$  = absorptivity of the gases at  $T_w$ ,

$T_g$  = absolute temperature of gases, K,

- Convective heat transfer from gases to wall,

$$q_{gas} = h(T_g - T_w)$$

where:

$h$  = coefficient of heat transfer by convection from gases to the combustor wall,

Under steady state condition assuming the total rates of heat flow is the same through the gases medium in the combustor and the metal medium of the heat flux meter. The total heat transfer to the combustor wall could be given by:

$$q_{total} = q_{R-flame} + q_{R-gas} + q_{Convected\ gas}$$

$$= \text{constant}_1 (T_p^4 - T_w^4) + \text{constant}_2 (T_g^4 - T_w^4) + \text{constant}_3 (T_g - T_w)$$

Assuming  $T_p = T_g$ , the right side of the above equation can be reduced to

$$q_{total} = \text{constant} (T_g - T_w)$$

$$= h_{R-C} (T_g - T_w)$$

where:

$h_{R-C}$  = radiant-convective overall heat transfer coefficient.

By equating the above equation to the total heat transfer through the heat flux meter,

$$q_{total} = h_{R-C} (T_g - T_w)$$

$$= \text{heat flux} = \frac{k \cdot \Delta T_x}{x} \quad W/m^2$$

where:

$k$  = thermal conductivity of heat flux meter metal (steel, 49 W/m. $^{\circ}$ C)

$\Delta T_x$  = differential temperature along the heat flux meter,  $^{\circ}$ C

$x$  = longitudinal distance, (0.05 m)

$$\therefore h_{R-C} = \frac{k \cdot \Delta T_x}{x \cdot (T_g - T_w)} \quad W/m^2 \cdot ^{\circ}C$$

### 3.2. Combustion Level

Ash mixture of the collected fly-ash and the bed-ash is formed. This mixture is composed of a proportional gravimetric percentage of each ash. The total combustion level fraction is determined by ashed the prepared mixture (used ash as a tracer) to determine how much combustibles percent are lost using the following relation [18]:

$$\text{Combustion level} = \frac{\left( \frac{1 - A_o}{A} \right)}{(1 - A_o)} \quad \%$$

where:

$A_o$  = initial ash percent.

$A$  = ash percent at a certain section.

This expression is a measure of the combustible mass loss of the solid material produced by devolatilization and char reaction. Ash weight percent is determined by using an electrical oven and an electronic balance.

### 4. FLUIDIZATION PROCESS AND PARTICLES COMBUSTION

A simulated transparent vessel is prepared, Fig.2, to study the fluidization process using colored plastic particles instead of coal. As air is blown upward through the distribution plate, bubbles are formed above the plate and rise up with growing in size. When the buoyancy force is sufficient to overcome the weight of the particles, the particles bed is suspended in the air stream. As soon as maximum bubbles sizes are formed, they became unstable and split out. Further increase in the air velocity, creation of "bubbling" within the vessel is increased and occurred very similar to that of the boiling water. This fluidization generates tremendous turbulence within the bed resulting in significant mixing of particles with air. That is considered a very good characteristic for coal particles combustion.

When air temperature at the fluidized bed is reached 500 $^{\circ}$ C, the coal

particles are fed to the bed and mixed with the hot combustion air. One of the four gas burners is re-lighted and only used to ignite the coal particles. Consequently, the coal particles are dried and then devolatilized - driving off- the brown volatile matters which are burnt and forming floating flames on the bed surface. The flames are extended up to the end of the free board and occupied most the combustor vessel. Unconfined volatiles flame is shown in Fig.3-A. After the evolution of the volatile matters is stopped, the flames are dragged down toward the bed where the remaining char-coal particles are oxidized within the bed for longer period forming very luminous flames. Unconfined char flame is shown in Fig.3-B.

Shattering is happened for the coal particles due to the effect of the thermal stress and the increase of the internal pressure [19]. This is applicable most for big particles, in particular for the tested size 17 mm. There is further breakage termed "attrition" which is occurred as a result of particles-particles and particles-fixed surface collisions. This causes hastening particles combustion leading to an increase of gas temperatures in the bed and free board.

## 5. DISCUSSION OF THE EXPERIMENTAL RESULTS

For the bubbling fluidized bed combustor; gas temperature distributions, heat transfer to the combustor wall, and combustion level of the coal particles are investigated experimentally for the different particles size at constant fluidized air velocity of 1.0 m/s.

### 5.1. Gas Temperatures

Coal particles with different size of 1.7, 3.7, 5.5, 9, and 17 mm are fed onto the distributor plate meanwhile the hot combustion air is blown upward with a small beginning velocity which is increased gradually until it reaches 1.0 m/s. After ignition, coal particles combustion is phenomenally by two main regimes: the combustion of volatile matters regime which

is extended from the bed to the free board, and the char-coal regime which is occurred mainly within the bed. Gas temperatures along the free board at centerline and wall during the two regimes are measured and plotted as profiles in Figs.4-7

For the devolatilization combustion regime, Figs.4 and 5, it is found that the centerline and near wall gas temperatures at the fluidized bed surface (at bed vertical distance/bed width, ratio  $L/w = 0.9, 1.2$ ) are found to be the maximum values which are decreased by moving upward, away from the fluidized bed surface. Except for the coal particles size 17 mm, the gas temperatures are increased gradually until reach the maximum values at  $L/w = 2.1$ , where the amount of the released volatile matters are bigger and seems to have heavier molecules. So the volatiles matter takes longer time to be break down into lighter molecules which are burnt later downstream. As coal particle sizes are decreased, the gas temperatures at centerline and wall are increased. The highest temperatures are found to be for particles diameter 1.7 mm while the lowest for particles diameter 17 mm. The temperatures trend at centerline is matched-up with those at wall. The average gas temperature along the free board at the centerline is found to be 875°C for small particle sizes (1.7, 3.7, and 5.5 mm) while it is 575°C for bigger particle sizes (9.0 and 17 mm). The average values at wall are found to be 680°C for the small particles and 350°C for the big particles respectively.

For the char-coal reactivity regime, Figs.6 and 7, the reaction is transferred from diffusion control to chemical control. As coal particles size is increased from 1.7 to 3.7 and 5.5 mm, the centerline and wall gas temperature values along the free board section are decreased. But, further increase in the particles size to 9 and 17 mm leads to an increase in the gas temperature values. The maximum values are found to be for particles size 17 mm, where at that size the particles are shattered for smaller particles and the remainder volatile matters have

more opportunity to escape and to enhance the reaction. The average gas temperature along the centerline free board is 720°C for small particles while for big particles size it is 900°C and the corresponding values at wall are 620°C and 700°C, respectively.

It is noticed that the overall average gas temperatures along the free board for char-coal reactivity regime is higher than that for volatile matters combustion regime.

### 5.2. Heat Transfer to the Combustor Wall

Heat flux,  $\text{KW/m}^2$ , to the combustor wall is deduced from the temperature difference which, are measured along the heat flux meter. In general, the largest values of heat flux are found to be near the bed surface. Moving away to the upper direction, the values are decreased as shown in Figs.8 -11.

For the devolatilization regime, Figs.8 and 9, as coal particles size is increased from 1.7 mm to 3.7, 5.5, 9, and 17 mm the heat flux and the radiant-convective overall heat transfer coefficient ( $h_{R-C}$ ) values are decreased. The maximum average value of heat flux is 142  $\text{KW/m}^2$ , and the maximum radiant-convective overall heat transfer is 1070  $\text{W/m}^2\cdot^\circ\text{C}$  which, are found to be for the smallest particles size of 1.7 mm.

For the char-coal reactivity regime, Figs.10 and 11, the heat flux values are matching-up with the values of  $h_{R-C}$  and their descending order is corresponding to the particles sizes order of 17, 1.7, 3.7, 9, and 5.5 mm respectively. The maximum average value of heat flux and radiant-convective overall heat transfer coefficient are 142  $\text{KW/m}^2$  and 950  $\text{W/m}^2\cdot^\circ\text{C}$  respectively which are found to be for the largest particles size of 17 mm.

### 5.3. Combustion Level of the Coal Particles

The obtained results of the combustion level are presented in Fig.12. As coal particles size is increased from 1.7 mm to 3.7, 5.5, 9, and 17 mm the

corresponding combustion levels are 80%, 91%, 96%, 97% and 98% respectively. That is because smaller particles have more opportunity to escape with the flue gases without completion of combustion. So, for the highest demand of combustion level it is recommended to choose particles size of 17 mm and not less than 5.5 mm.

## 6. COMPARISON WITH WOOD COMBUSTION

Sawdust of a wood is collected and sieved to obtain available size of 0.7 mm. Also, coal is crushed and sieved to obtain the same size. A comparison between coal and wood combustion is held at constant fluidized air velocity of 1.0 m/s. For the case of coal combustion, mean values are considered (i.e. the mean value between the devolatilization regime and the char-coal regime) where wood has nearly one combustion regime.

For coal combustion, the behavior of gas temperatures along the centerline and near the wall is the same. The highest values at centerline and wall are 1170°C and 960°C respectively, which are found to be near the bed as shown in Fig.13. Moving upward away from the bed, the temperatures are decreased. The average gas temperature values along the combustor at centerline and wall are 980°C and 830°C respectively. The temperature difference of the gas at centerline and wall along the combustor is kept constant at about 130°C. The radiant-convective overall heat transfer coefficient has the same trend of gas temperatures as shown in Fig.14. The maximum value of  $h_{R-C}$  is 1420  $\text{W/m}^2\cdot^\circ\text{C}$ , and the average value along the free board is about 1050  $\text{W/m}^2\cdot^\circ\text{C}$ . The coal particles of 0.7 mm are burnt, mostly, at the free board because their buoyancy force is higher than their weight. As a result these particles have more opportunity to escape without complete combustion and causing a reduction of combustion level to 64%.

For wood combustion flames which shown in Fig.15, the behavior of gas temperatures at centerline and wall is the

same, both of them are increased gradually up to certain value and kept nearly constant then decreased gradually at the end of the free board, Fig.13. The influence of the thermal response of wood combustion is delayed, that shifted the maximum gas temperature downstream away from the bed. The difference between the gas temperatures at centerline and near the wall along the free board is kept constant at about 400°C. This big difference could be due to the little heat released of wood combustion which is not enough to compensate the losses of heat to surrounding. As a result, the gas temperatures at wall are low and consequently the average value of the radiant-convective overall heat transfer coefficient along the free board is too low and equal to 200 W/m<sup>2</sup>.°C, as shown in Fig.14.

It is noticed that, for coal combustion the average gas temperatures along the free board at centerline is greater than those for wood combustion by 170°C, and this difference at wall is 450°C. Also, the average radiant-convective overall heat transfer coefficient ( $h_{R-C}$ ) for coal combustion is 5 times of that of wood combustion.

## 7. CONCLUSIONS

1. The designed system is valid to burn solids, coal and wood particles, properly and efficiently.
2. The combustion mechanism of the fluidized coal particles is phenomenally by two combustion regimes; the devolatilization and the char regimes.
3. As coal particle sizes are increased from 1.7 to 3.7, 5.5, 9, and 17 mm, during the devolatilization regime, the gas temperatures at centerline and wall are decreased. The average gas temperatures along the combustor at centerline and wall for small particles size (1.7, 3.7 and 5.5 mm) are 875°C and 680°C respectively. For large particles size (9 and 17 mm) the corresponding temperatures are 575°C and 350°C respectively. While during the char regime, the average gas temperatures for the small particles are 720°C and 620°C respectively and for large particles are 900°C and 700°C respectively. The overall average gas temperature along the combustor for char regime is higher than that for devolatilization regime.
4. As coal particle sizes are increased from 1.7 to 3.7, 5.5, 9, and 17 mm, during the devolatilization regime, the heat flux and the radiant-convective overall heat transfer coefficient ( $h_{R-C}$ ) to the combustor wall, are decreased. The maximum average values of the heat flux and the overall heat transfer coefficient are found to be for the smallest particles size 1.7 mm and their values are 142 KW/m<sup>2</sup> and 1070 W/m<sup>2</sup>.C respectively. While during the char regime, the maximum corresponding average values are found to be for the biggest coal particles size 17 mm and their values are 142 KW/m<sup>2</sup> and 950 W/m<sup>2</sup>.C respectively.
5. As coal particle sizes are increased from 0.7, to 1.7, 3.7, 5.5, 9, and 17 mm the obtained combustion levels are increased from 64% to 80%, 91%, 96%, 97% and 98% respectively. Hence for the highest demand of combustion level it is recommended to choose particles size 17 mm and not less than 5.5 mm.
6. A comparison is held between coal and wood combustion for the same particles size of 0.7 mm. For coal combustion, the average gas temperatures along the combustor at centerline and wall are 980°C and 830°C respectively, and the average value of radiant-convective overall heat transfer  $h_{R-C}$  is 1050 W/m<sup>2</sup>.°C.

For wood combustion, the produced gas temperatures values are lower as well as  $h_{R-C}$  which has a value of  $200 \text{ W/m}^2\cdot\text{C}$  (i.e. one fifth of the corresponding value of coal combustion).

## 8. REFERENCES

1. Akira Nakamura, Toshihiko Lwasaki, Takashi Noto, Hisanao Hashimoto, Nobuyuki Sugiyama, and Masahiro Hattori, NKK Technical Review No.86, pp: 30-35, 2002.
2. V.I.Kuprianov, K.Janvijitsakul and W.Permchart, Fuel, Volume 85, issue 4, pp: 434-442, March 2006.
3. Skinner, D.G., National Coal Board Research and Development (CPC), January, 1970.
4. Koommeef, J., M. Junginger, and A. Faaij., Progress in Energy and Combustion Science, 33, pp: 19-55, 2007.
5. Elliot, M.A. (ed.).Chemistry of Coal Utilization, secondary suppl. New York: Jon Wiley & Sons, 1981.
6. Saha, S.N., Fuel Combustion Energy Technology, Kapur, K.K., DELHI, 2003.
7. Rowe P N, Partridge B A, Cheney A G, Henwood G A, Lyall E. Trans. Inst. Chem. Eng., Volume 32, T271-T286, 1965.
8. Davies L and Richardson J F, Trans. Inst. Chem. Eng. Volume 44, T293-T305, 1966.
9. J.M. Sanchez-Hervas, L. Armesto, E. Ruiz-Martinez, J. Otero-Ruiz, M. Pandelova and Scramm K.W., Fuel, volume 84, issue 17, pp: 2149-2157, December 2005.
10. Raymond C Everson, Hein W.J.P. Neomagus, Henry Kasaini and Delani Njapha, Fuel, volume 85, issues 7-8, pp: 1067-1075, May 2006.
11. Aly Kamel Abd El-Samed, PSERJ, Vol.10, No.1, pp: 74-91, March 2006.
12. Lufei Jia, Edward J. Anthony, Ivan Lau and Jinsheng Wang, Fuel, Volume 85, issues 5-6, pp: 635-642, March-April, 2006.
13. Jansson, S.A., Eighth Int. Conf. On Fluidized Bed Combustion, Houston, Texas, paper 9.5, 1985.
14. Ellis, F. Eighth Int. Conf. On Fluidized Bed Combustion, Houston, Texas, paper 17.2, 1985.
15. Stringer, J and Minchener, A.J., Conf. Fluidized Combustion, Inst. Of Energy, London, paper DISC/29, 1984.
16. Minchener, A.J. and Stringer, J., J. Inst.Energy volume 57, pp: 240-251, 1984.
17. Wu, Z, understanding fluidized-bed combustion: IEA coal research, 2003.
18. Aly K. Abd El-Samed, Eighth Int.Conf.Mech. Power Eng., Vol.1, pp: 495-513, Alexandria, Egypt, April 27-29, 1993.
19. Aly K.Abd El-Samed, E.Hampartsomium, T.M.Farag, and A. Williams, Fuel, Vol.69, pp: 1029-1036, 1990.



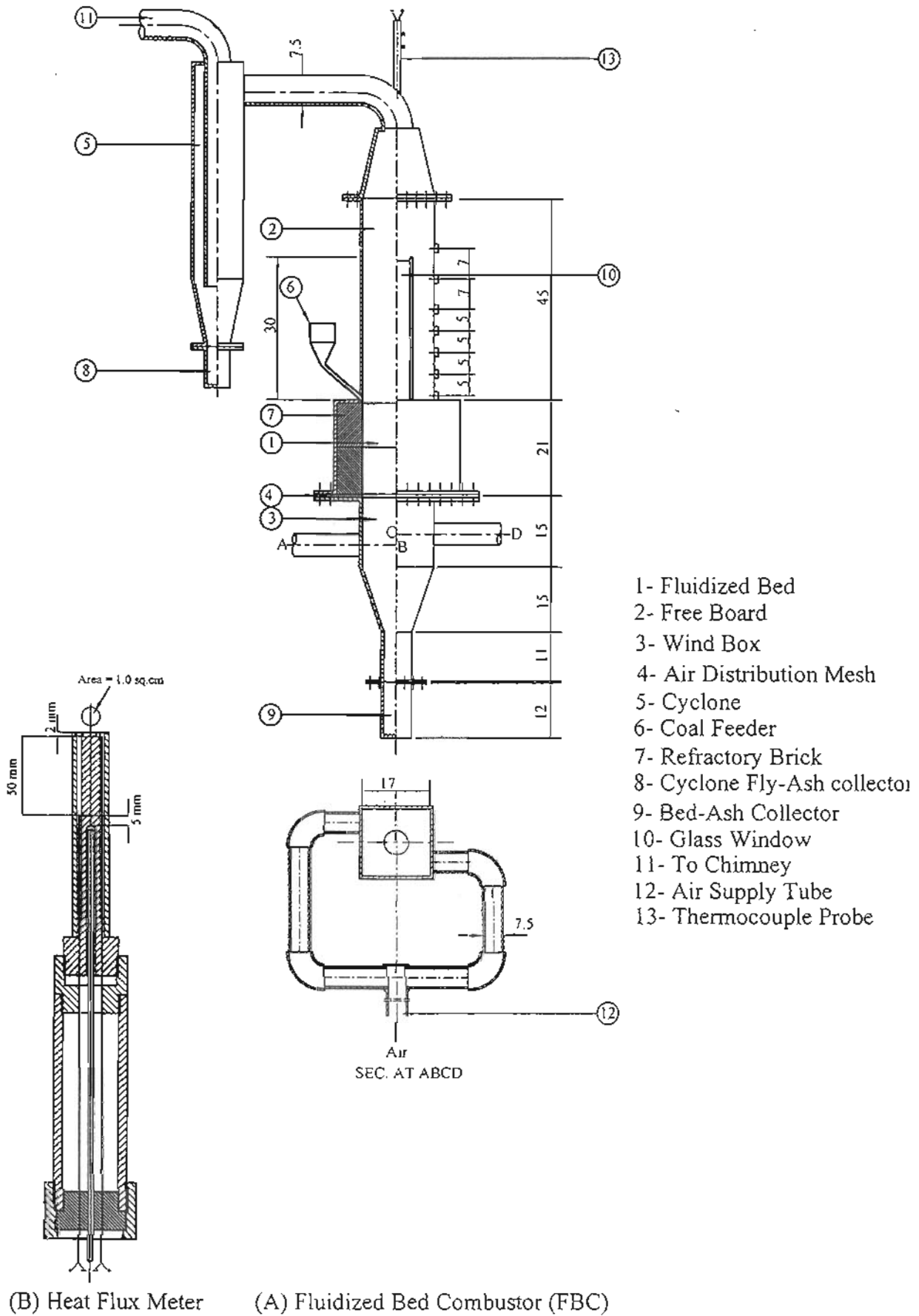


*Fig.1 Fluidized Bed Apparatus*



Fig.2 Simulation of fluidization process

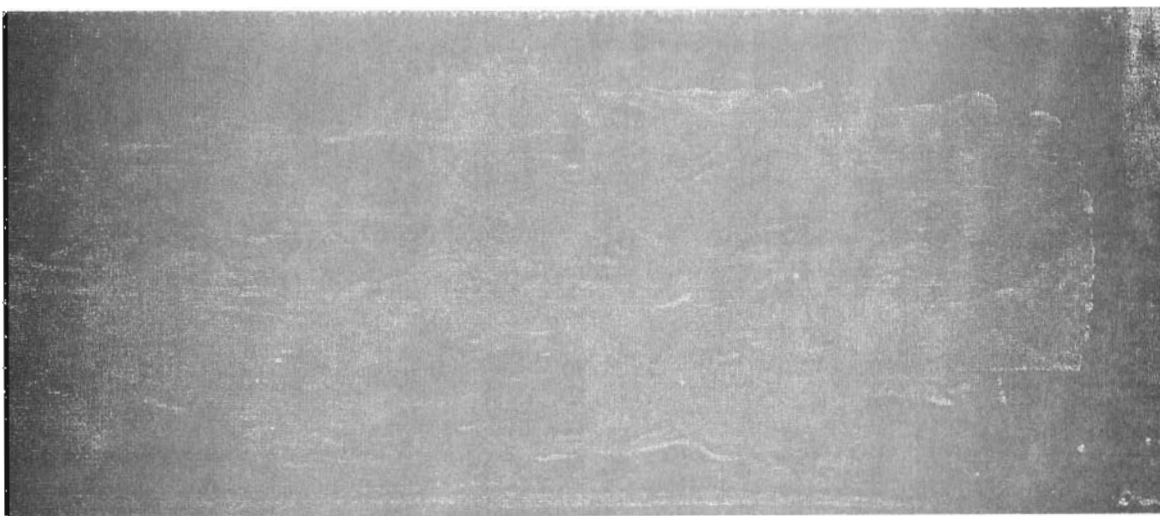


Fig.3-A Unconfined volatiles flame

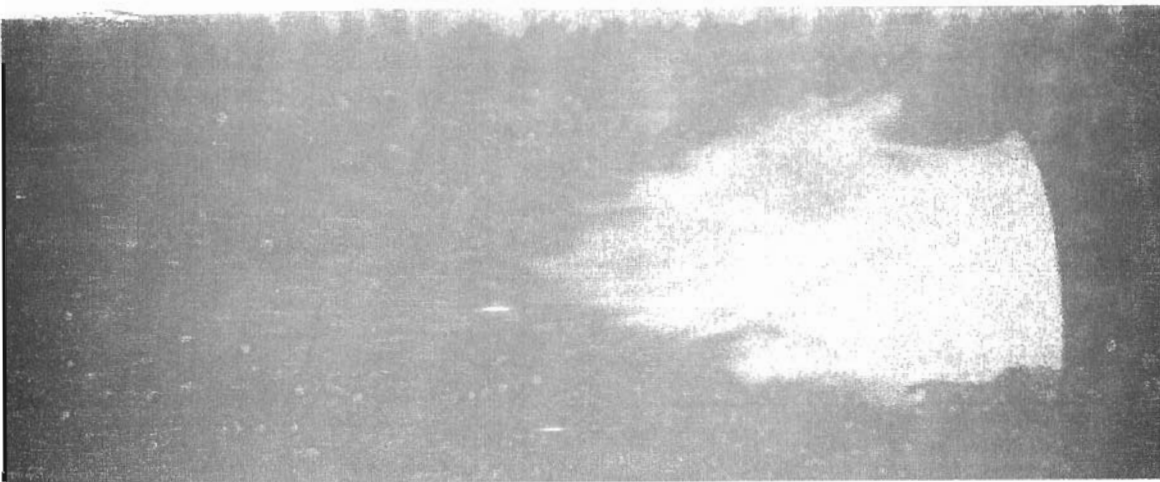


Fig.3-B Unconfined char flame

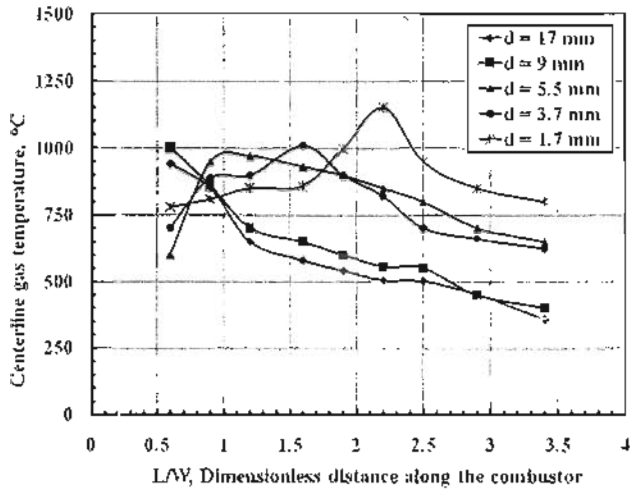


Fig.4 Gas temperature distribution along the combustor centerline, during the devolatilization regime.

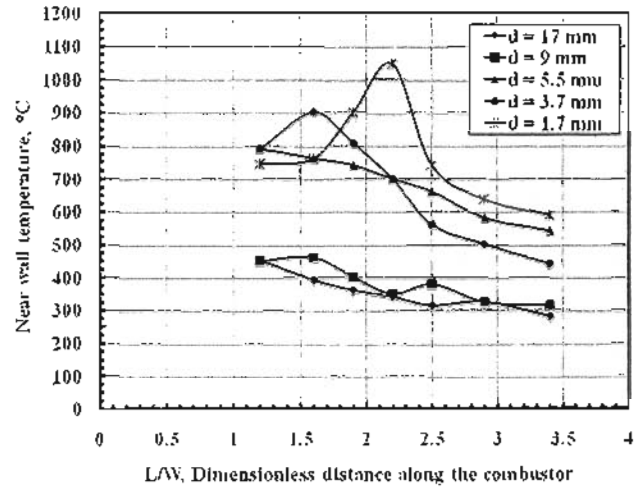


Fig.5 Gas temperature distribution along the combustor wall, during the devolatilization regime.

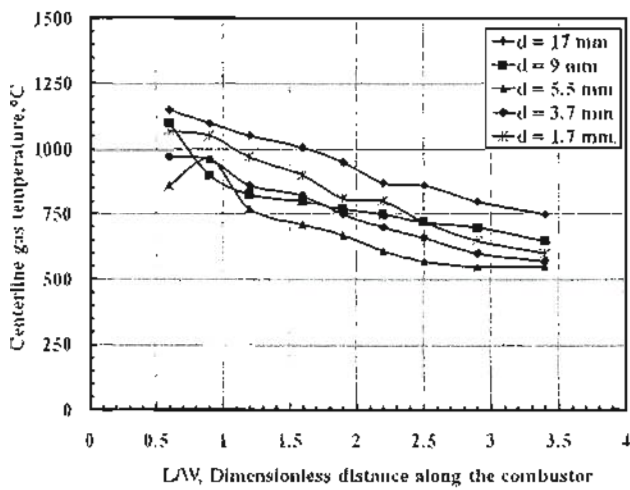


Fig.6 Gas temperature distribution along the combustor centerline, during the char combustion regime.

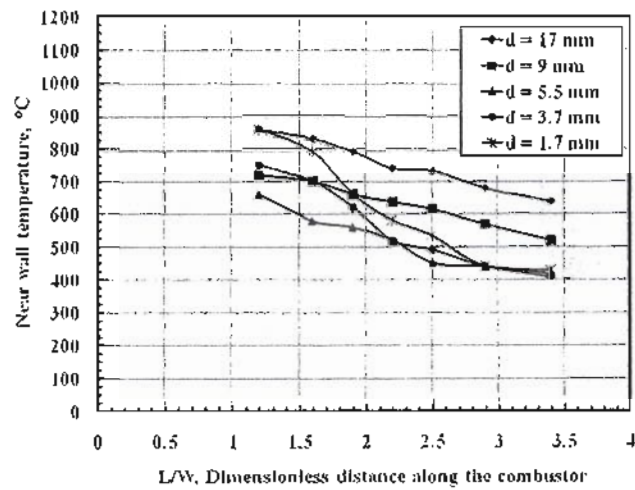


Fig.7 Gas temperature distribution along the combustor wall, during the char combustion regime.

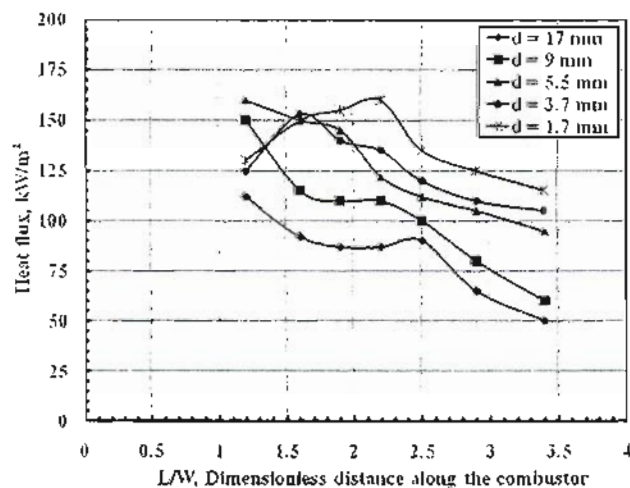


Fig.8 Heat flux distribution along the combustor, during the devolatilization regime.

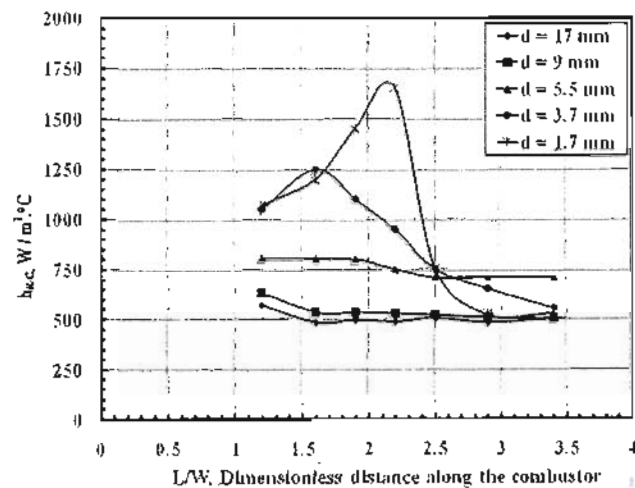


Fig.9 Radiant convective overall heat transfer coefficient ( $h_{r,c}$ ), during the devolatilization regime.

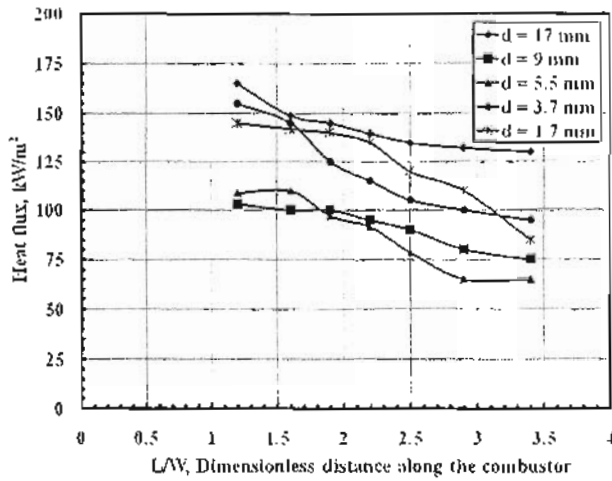


Fig.10 Heat flux distribution along the combustor, during the char combustion regime.

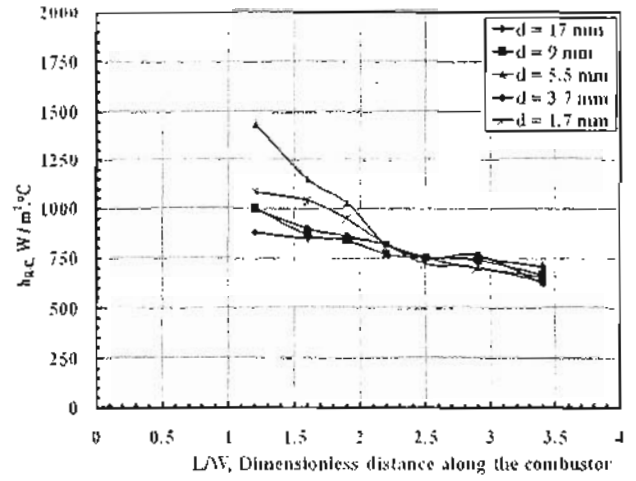


Fig.11 Radiant convective overall heat transfer coefficient ( $h_{R-C}$ ), during the char combustion regime.

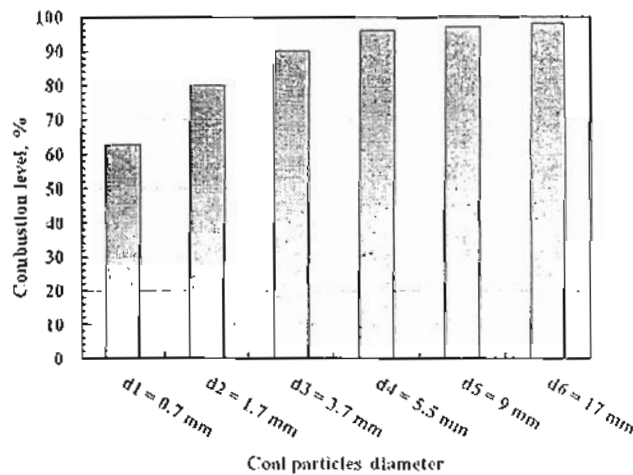


Fig.12 Combustion level for different coal particles size

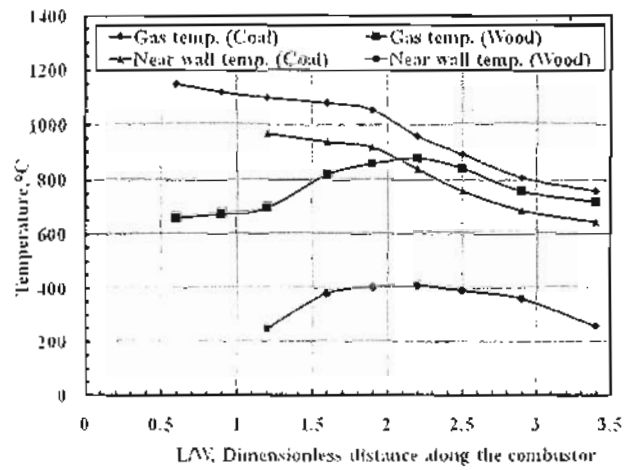


Fig.13 Gas temperature distributions at centerline and near wall for coal and wood combustion

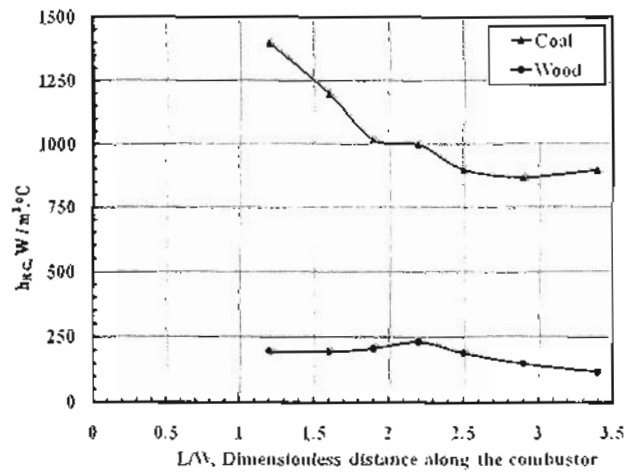


Fig.14 Radiant-convective overall heat transfer coefficient ( $h_{R-C}$ ) for coal and wood combustion



Fig.15 Unconfined wood combustion flame